Flash Photolysis Studies of the Reactions of Dinuclear Manganese Carbonyl Compounds with Tributyltin Hydride and Triethylsilane

Richard J. Sullivan and Theodore L. Brown*

Contribution from the School of Chemical Sciences, University of Illinois, Urbana-Champaign, Illinois 61801. *Received February 27, 1991. Revised Manuscript Received July 19, 1991*

Abstract: The reactions of $Mn_2(CO)_8L_2$ (L = CO, PMe_3, $P(n\text{-}Bu)_3$, $P(i\text{-}Bu)_3$, $P(i\text{-}Pr)_3$, $P(C_6H_{11})_3$) with $HSnBu_3$ and of $Mn_2(CO)_{10}$ with $HSiEt_3$ were studied via flash photolysis, employing a conventional xenon flash lamp apparatus. The flash photolysis results are consistent with the conclusions based on continuous photolysis studies. The predominant reaction involves oxidative addition of the hydride to manganese at the site of CO loss. The rate of oxidative addition decreases as the steric requirements of L increase. Following oxidative addition, reductive elimination occurs. For $HSnBu_3$, $HMn(CO)_4L$ and $Bu_3SnMn(CO)_3L$ are formed. In the reaction of $HSiEt_3$ with $Mn_2(CO)_{10}$, reformation of $HSiEt_3$ dominates over formation of $HMn(CO)_5$. The lifetime of the intermediate product resulting from the initial addition varies greatly with L. For small L, such as CO or PMe_3, the intermediate persists for several seconds. With increasing size of L the addition process is slowed and the rate of elimination increases. A complete model for the reaction systems takes account of the semibridging form of the CO-loss product as the prevalent species in a noncoordinating solvent. Detailed modeling of the reaction system indicates that the on–off equilibrium involving coordination of the semibridging CO to the vacant manganese site is kinetically important. Formation of the semibridging form from the open form appears to have a significant energy barrier.

In the preceding paper in this issue, we presented evidence that the photochemical reaction of dinuclear manganese carbonyl compounds with tributyltin hydride or triethylsilane occurs via oxidative addition to the primary photochemical product resulting from CO loss.[1] However, the details of the reaction could not be determined from continuous photolysis studies. From prior photochemical studies of $Mn_2(CO)_{10}$,[2-9] and from studies of the products of photochemical CO loss from mononuclear metal carbonyl compounds,[10-15] the presences of various intermediates preceding oxidative addition to the dinuclear intermediates can be inferred. In addition, aside from their eventual fates, intermediates resulting from addition of the hydride may have significant lifetimes. Accordingly, we have carried out flash photolysis studies of the photochemical reactions of $Mn_2(CO)_8L_2$ (L = CO, PMe_3, $P(n\text{-}Bu)_3$, $P(i\text{-}Bu)_3$, $P(i\text{-}Pr)_3$, $P(C_6H_{11})_3$) with $HSnBu_3$ or $HSiEt_3$, with the aim of attaining a more complete understanding of the overall reaction processes.

Meyer and co-workers were the first to note that photolysis of $Mn_2(CO)_{10}$ produces two photoproducts, the $Mn(CO)_5$• radical, formed by Mn–Mn bond homolysis, and $Mn_2(CO)_9$, formed by CO loss.[3] Subsequent laser flash photolysis studies have confirmed the natures of the two photoproducts.[4,5] By analogy with the properties observed for $Cr(CO)_5$,[10-13] the immediate product of CO loss should undergo solvation within 100 ps to form $Mn_2(CO)_9(S)$ (S = solvent). However, $Mn_2(CO)_9$ differs from the mononuclear species in that it adopts a semibridging structure, I.

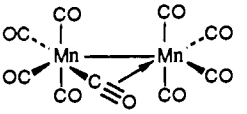

The existence of this species in solution was first proposed by Hepp and Wrighton,[6] on the basis IR evidence and the analogy to $Mn_2(CO)_5(dppe)_2$[16] in which a stable semibridging arrangement is evident in the solid-state structure. It has also been observed as a product of photochemical CO loss in a matrix at 12 K.[7] Subsequently, it was observed in hydrocarbon solution at room temperature, through transient IR spectroscopic studies.[8] Neither the energetics nor kinetics of its formation are known. The bimolecular rate constant for addition of CO to $Mn_2(CO)_9$, presumably in the semibridging form, is about 2.9×10^5 M^{-1} s^{-1}.[8,17a] (2.4×10^6 M^{-1} s^{-1} in the gas phase).[17b] This is not much less than the value of 3×10^6 M^{-1} s^{-1} observed for the analogous reaction at $Cr(CO)_5$. The rate of the latter process is limited by the dissociation of solvent from $Cr(CO)_5(S)$, whereas in the former it is presumably limited by the rate of dissociation of the semibridging CO from the site of unsaturation. Significantly, the rate constant for CO addition to $Mn_2(CO)_9$ in perfluoroalkane solvent is about the same as in hexane,[17a] whereas it is about 10^3 faster for CO addition to $Cr(CO)_5$ in perfluoroalkane as contrasted with alkane solvent.[14b] The difference in the two systems may reflect the free energy barrier arising from stabilization of the semibridging form over the "naked" metal center in the dinuclear compound.

In this paper we report several new observations that have important implications for the photochemical behaviors of the manganese carbonyl/metal hydride systems in the presences of

(1) Sullivan, R. J.; Brown, T. L. *J. Am. Chem. Soc.*, preceding paper in this issue.
(2) Meyer, T. J.; Caspar, J. V. *Chem. Rev.* **1985**, *85*, 187.
(3) Hughey, J. L.; Anderson, C. P.; Meyer, T. J. *J. Organomet. Chem.* **1977**, *125*, C49.
(4) (a) Rothberg, L. S.; Cooper, N. J.; Peters, K. S.; Vaida, V. *J. Am. Chem. Soc.* **1982**, *104*, 3536. (b) Leopold, D. G.; Vaida, V. *J. Am. Chem. Soc.* **1984**, *106*, 3720. (c) Prinslow, D. A.; Vaida, V. *J. Am. Chem. Soc.* **1987**, *109*, 5097.
(5) Yesaka, H.; Kobayashi, T.; Yasufuku, K.; Nagakura, S. *J. Am. Chem. Soc.* **1983**, *105*, 6249.
(6) Hepp, A. F.; Wrighton, M. S. *J. Am. Chem. Soc.* **1983**, *105*, 5934.
(7) Dunkin, I. A.; Härter, P.; Shields, C. J. *J. Am. Chem. Soc.* **1984**, *106*, 7248.
(8) Church, S. P.; Hermann, H.; Grevels, F.-G.; Shaffner, K. *J. Chem. Soc., Chem. Commun.* **1984**, 785.
(9) Kobayashi, T.; Ohtani, H.; Noda, H.; Teretani, S.; Yamazaki, H.; Yasufuku, K. *Organometallics* **1986**, *5*, 110.
(10) (a) Simon, J. D.; Peters, K. S. *Chem. Phys. Lett.* **1983**, *90*, 6751. (b) Simon, J. D.; Xei, X. *J. Phys. Chem.* **1986**, *90*, 6751. (c) Xie, X.; Simon, J. D. *J. Am. Chem. Soc.* **1990**, *112*, 1130. (d) O'Driscoll, E.; Simon, J. D. *J. Am. Chem. Soc.* **1990**, *112*, 6580.
(11) Joly, A. G.; Nelson, K. A. *J. Phys. Chem.* **1989**, *93*, 2976.
(12) (a) Wong, L.; Zhu, X.; Spears, K. G. *J. Am. Chem. Soc.* **1988**, *110*, 8695. (b) Wong, L.; Zhu, X.; Spears, K. G. *J. Phys. Chem.* **1989**, *93*, 2.
(13) Lee, M.; Harris, C. B. *J. Am. Chem. Soc.* **1989**, *111*, 8963.
(14) (a) Kelly, J. M.; Bent, D. V.; Hermann, H.; Schulte-Frohlinde, D.; Koerner von Gustorf, E. A. *J. Organomet. Chem.* **1974**, *69*, 259. (b) Bonneau, R.; Kelly, J. M. *J. Am. Chem. Soc.* **1980**, *102*, 1220. (c) Kelly, J. M.; Long, C.; Bonneau, R. *J. Phys. Chem.* **1983**, *87*, 3344.
(15) (a) Zhang, S.; Dobson, G. R. *Inorg. Chem.* **1989**, *28*, 324. (b) Dobson, G. R.; Zhang, S. *J. Coord. Chem.* **1990**, *21*, 155.
(16) Commons, C. J.; Hoskins, B. F. *Aust. J. Chem.* **1975**, *28*, 1163.
(17) (a) Herrick, R. S.; Brown, T. L. *Inorg. Chem.* **1984**, *23*, 4550. (b) Seder, T. A.; Church, S. P.; Weitz, E. *J. Am. Chem. Soc.* **1986**, *108*, 7518.

0002-7863/91/1513-9162$02.50/0

potential substrates. Among these is the observation that the intermediates resulting from addition of the metal hydride to $Mn_2(CO)_9$, or to the less hindered of the bis(phosphine)-substituted dimers, are quite long-lived. They persist for periods of from 1 to $>10^2$ s, during which time they are available for reaction with substrates.

Secondly, the kinetic behavior of the oxidative addition of $HSnBu_3$ to $Mn_2(CO)_8(PMe_3)_2$ and $Mn_2(CO)_8[P(n\text{-}Bu)_3]_2$ can be interpreted in terms of a rate-limiting equilibrium between the semibridged and unbridged, or open, form of $Mn_2(CO)_8L_2$. The detailed kinetics of the addition reaction, coupled with numerical simulations of the reaction system, indicate that a barrier, other than that associated with dissociation of solvent from the reaction site, exists for formation of the semibridged species.

Experimental Section

Materials. Solvents and reagents were acquired, prepared and handled as described in the previous paper in this issue.[1] Bis(phosphine)-substituted compounds $Mn_2(CO)_8L_2$ were prepared by the same procedures described there; all gave satisfactory elemental analyses, and exhibited characteristic IR spectra free of evident impurities.

Flash Photolysis Apparatus. The flash photolysis apparatus employed consisted of linear Xe flash lamps (EG&G FX-142C-4.5), connected in series to a high-voltage power supply and electrical discharge system. The major features of the apparatus have been described elsewhere.[18] Typically, the maximum intensity of light in the flash occurs about 13 μs after initiation of the discharge; the half-intensity width ranges around 30 μs, and the radiative afterglow has completely ceased after about 100 μs.

The detection system consists of a Ushio or Osram 100-W, 12-V quartz–halogen tungsten filament lamp, mounted in an Illumination Industries Model LH353Q lamp housing. The lamp is powered by a Schoeffel Instruments, Inc., Model 1152/1144 universal arc lamp power supply. An electronic shutter (Uniblitz) is used to block the probe beam from the sample until the flash event. Typically, a 470-nm long-pass filter is placed between the lamp and sample cell to cut off short-wavelength light. The probe beam, after passing through the solution, is passed through a 200-mm focal length monochromator and then to a thermoelectrically cooled photomultiplier tube holder fitted with a Hamamatsu R928 photomultiplier tube (peak response at 400 nm). (The R928 is a good choice for the work described here, because it has sufficient response at long wavelength to enable observation of the transient absorptions due to $Mn(CO)_4L^*$ radicals, which absorb in the 700–800-nm region, as well as $Mn_2(CO)_7L_2$, which have absorption maxima in the vicinity of 500 nm.) Following amplification, the signal is sent to a Markenrich WAAG high-speed data acquisition board, capable of collecting 2000 8-bit data points, at sampling rates from 0.5 ms to 0.5 μs per channel. The board is mounted in an AST Premium 286 AT class computer. Data manipulation and analysis are performed using mainly the ASYST software package.

Flash Photolysis Procedures. Solutions were prepared under an Ar atmosphere in a glovebox. The solutions were then placed in the cells employed for flash photolysis. These consist of a cylindrical sample chamber about 10 cm in length, and of 2.5-cm diameter, fabricated of Pyrex, an attached bulb in which the solutions can be frozen and degassed, and a stopcock that provides a vacuum-tight seal. The dimensions of the cells and concentrations employed are such that the contents of the sample chamber are subjected to a nearly uniform flux of photons during the flash. Thus, there should be no significant concentration gradients established during the photolysis.

The cells could be pressurized with CO gas up to a few atmospheres by attaching the cell to a manifold, degassing, and then admitting CO to the desired pressure. Experiments were conducted at ambient room temperature, normally about 22 °C. To observe the transient absorption of each CO loss product, a wavelength in the range from 510 to 560 nm was chosen, to optimize the difference in absorbances between the semibridged CO-loss species[17a] and the adduct resulting from reaction with hydride.

Results

A. Reactions of $Mn_2(CO)_8L_2$ with $HSnBu_3$. $Mn_2(CO)_{10}$. When $Mn_2(CO)_{10}$ in hexane solution is flash-photolyzed, a transient absorption appears with absorption maximum at 510 nm. In solutions under Ar the transient disappears over a period of about 0.8 s, following a second-order rate law. Under added CO the disappearance occurs in a period on the order of milliseconds, and follows a pseudo-first-order rate law. The transient is assigned to $Mn_2(CO)_9$; it is presumably the semibridged form, which we will henceforth designate as $Mn_2(CO)_9$*. When $Mn_2(CO)_{10}$ is flash-irradiated under an N_2 atmosphere, the initial absorption at 510 nm immediately following the flash increases over several milliseconds. This process observed in this time domain is presumably formation of $Mn_2(CO)_9N_2$, via displacement of the semibridging CO by N_2. This species in turn disappears over a period on the order of 1 s, as CO replaces the N_2.

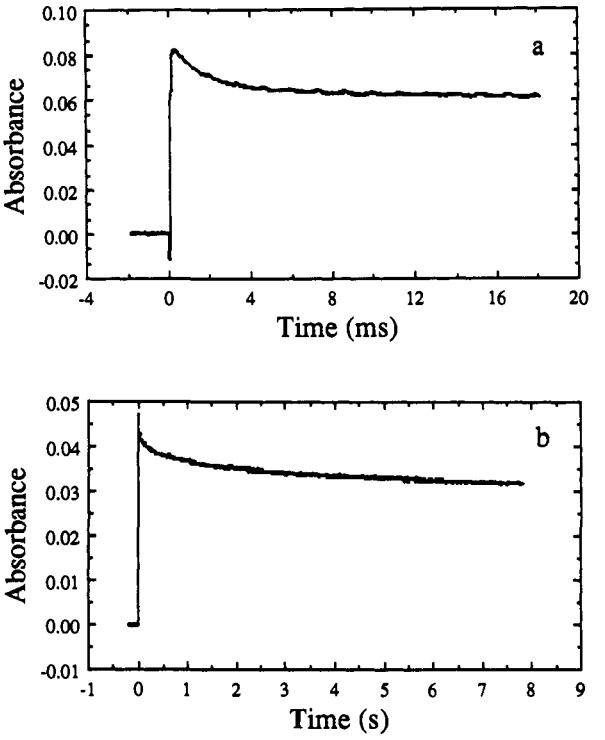

Figure 1. Transient absorption spectrum at 510 nm following flash photolysis of a hexane solution containing 1.0×10^{-4} M $Mn_2(CO)_{10}$ and 6.9×10^{-4} M $HSnBu_3$: (a) millisecond time domain; (b) longer time domain.

When $HSnBu_3$ is present in solutions at concentrations on the order of 10^{-2}–10^{-3} M in solutions under Ar, the initial absorbance decays in a few milliseconds to a new absorbance level about 80% as great as the initial value, as illustrated in Figure 1a. The intermediate giving rise to this absorbance in turn decays comparatively much more slowly. Figure 1b shows the decay over 8 s, the longest time scale available on our apparatus. It requires several minutes for the absorbance to return to the baseline.

Because the long-lived intermediate persists over several minutes, it was possible to obtain its FT-IR spectrum. After a solution of $Mn_2(CO)_{10}$ and $HSnBu_3$ was flash photolyzed in a 1-mm path length IR cell with KCl windows, a single FT-IR scan was acquired within about 40 s, at a nominal resolution of 2 cm^{-1}. The spectrum reveals that about 20% of the initial $Mn_2(CO)_{10}$ has disappeared. The predominant new IR bands are ascribable to $HMn(CO)_5$ and $HMn(CO)_4(SnBu_3)_2$.[1] In addition, bands at 2025, 1999, and 1948 cm^{-1} are assigned to $(CO)_5Mn\text{-}Mn(CO)_4(H)(SnBu_3)$ on the basis of analogy to the spectrum of the stable compound $Re_2(CO)_9(HSiEtCl_2)$.[19] Over time, the latter bands disappear, replaced by additional intensity in the bands due to $HMn(CO)_5$ and $HMn(CO)_4(SnBu_3)_2$, and a small absorbance due to $Bu_3SnMn(CO)_5$.

Our interpretation of the results described is that the initial rapid change in absorbance in the presence of $HSnBu_3$ is due to replacement of the semibridging CO in $Mn_2(CO)_9$* by $HSnBu_3$, to form an oxidatively added adduct, $(CO)_5Mn\text{-}Mn(CO)_4(H)(SnBu_3)$. This intermediate has significant absorption in the 500-nm region; as a result the initial decline in absorbance fol-

(18) Walker, H. W.; Herrick, R. S.; Olsen, R. J.; Brown, T. L. *Inorg. Chem.* **1984**, *23*, 3748.

(19) Hoyano, J. K.; Graham, W. A. G. *Inorg. Chem.* **1972**, *11*, 1265.

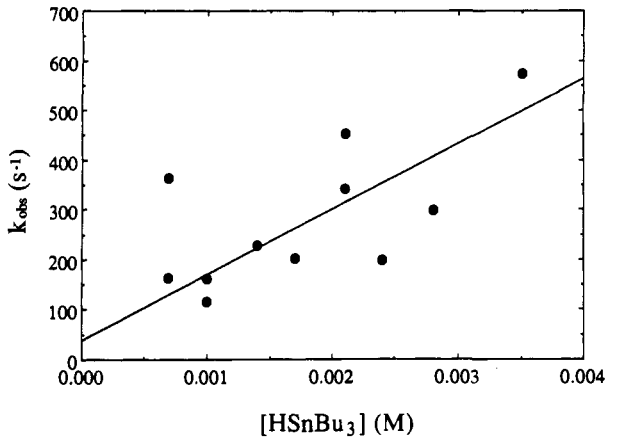

Figure 2. Pseudo-first-order rate constant, k_{obs}, for disappearance of the transient absorption assigned to $Mn_2(CO)_9$* as a function of $[HSnBu_3]$.

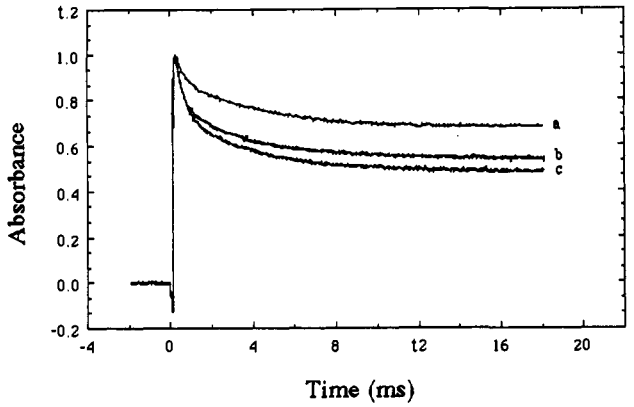

Figure 3. Normalized absorbance vs time plots for the decay of $Mn_2(CO)_9$* under 1.4 atm of CO for varying concentrations of $HSnBu_3$: (a) 4.2×10^{-3} M; (b) 2.1×10^{-3} M; (c) 6.9×10^{-4} M.

lowing the flash, which corresponds to oxidative addition, is relatively small (Figure 1a). The oxidative addition product eventually reductively eliminates $HMn(CO)_5$, leaving $Bu_3SnMn(CO)_4$. Under an Ar atmosphere, $Bu_3SnMn(CO)_4$ undergoes oxidative addition of $HSnBu_3$ to form $HMn(CO)_4(SnBu_3)_2$. It should be noted that there is no direct evidence from these results regarding the detailed nature of the bonding of $HSnBu_3$ to $Mn_2(CO)_9$; three-center, two-electron bonding[20] may play a role in the structure of the intermediate.

In the presence of added $HSnBu_3$, decay of the $Mn_2(CO)_9$* absorbance follows a first-order rate law. The pseudo-first-order rate constants, k_{obs}, could not be determined with good accuracy, however, because the change in absorbance is so small. A graph of k_{obs} vs $[HSnBu_3]$ is shown in Figure 2. The scatter is large, but the data appear to follow a linear relationship. From the slope, we obtain an estimate of the bimolecular rate constant for the reaction

$$Mn_2(CO)_9^* + HSnBu_3 \rightarrow (CO)_5Mn\text{-}Mn(CO)_4(H)(SnBu_3) \quad (1)$$

of about 1.3 (±0.5) × 10^5 M^{-1} s^{-1}. This value is more than 1 order of magnitude smaller than the value 3.0 × 10^6 M^{-1} s^{-1} estimated from the continuous photolysis studies.[1]

When CO is added to the system, it competes with $HSnBu_3$ for reaction with $Mn_2(CO)_9$*. As a result, the absorbance changes following the flash are larger, because the product of reaction with CO, $Mn_2(CO)_{10}$, does not absorb significantly in this region. Figure 3 shows the absorbance changes for three solutions, all under 1.4 atm of CO, for three different concentrations of $HSnBu_3$. From the absorbance changes in such experiments, it is possible to estimate the relative rate constants for reaction of $Mn_2(CO)_9$*

(20) Schubert, U. *Adv. Organomet. Chem.* **1990**, *30*, 151.

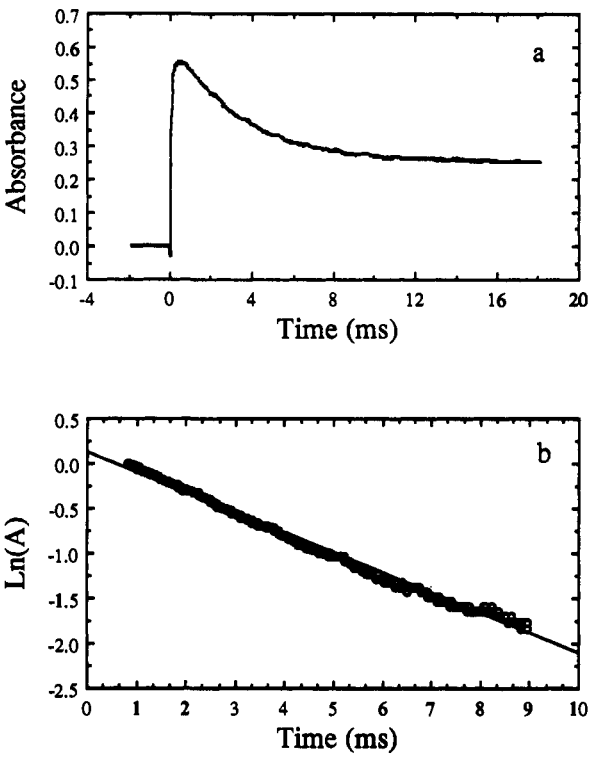

Figure 4. (a) Decay of the absorption at 530 nm following flash photolysis of 1.0×10^{-4} M $Mn_2(CO)_8(PMe_3)_2$ and 1.4×10^{-3} M $HSnBu_3$ in hexane, under Ar. (b) ln *A* vs time for the absorbance data from (a), showing a first-order dependence.

with either CO or $HSnBu_3$. Assuming a value of 2.9×10^5 M^{-1} s^{-1} for the CO reaction,[17] we obtain approximately 5×10^6 M^{-1} s^{-1} for the rate constant of the $HSnBu_3$ reaction, in reasonable agreement with the estimate of 3×10^6 M^{-1} s^{-1} from the continuous photolysis studies.[1] The discrepancy in the different approaches to estimating the oxidative addition rate constant probably arises because of the comparatively poor quality of the estimate for the second-order rate constant from the slope in Figure 2.

The decay of the oxidative addition product appears to obey a first-order rate law. Under Ar, the rate constant is independent of the concentration of $HSnBu_3$; we obtained a value of 1.5 (±0.3) × 10^{-2} s^{-1}. Under 1.4 atm of CO in solutions containing 4.2×10^{-3} M $HSnBu_3$, the first-order rate constant was larger, 2.7×10^{-2} s^{-1}. This suggests that $(CO)_5Mn\text{-}Mn(CO)_4(H)(SnBu_3)$ may also reductively eliminate $HSnBu_3$ (that is, the reverse of the oxidative addition process). When both CO and $HSnBu_3$ are present to react with the $Mn_2(CO)_9$* thus formed, the reaction with CO would result in immediate loss of absorbance at 510 nm. When added CO is not present, only $HSnBu_3$ is present to react with the $Mn_2(CO)_9$*, so the reductive elimination of $HSnBu_3$ from $(CO)_5Mn\text{-}Mn(CO)_4(H)(SnBu_3)$ has no effect. The fact that the apparent rate constant is only slightly increased by the presence of CO in significant excess over $HSnBu_3$ indicates that the predominant mode of reductive elimination is that which yields $HMn(CO)_5$.

$Mn_2(CO)_8(PMe_3)_2$. The transient absorbance following flash photolysis solutions of $Mn_2(CO)_8(PMe_3)_2$ was monitored at 530 nm. Under Ar, with no added $HSnBu_3$, the transient absorbance behaved as expected for $Mn_2(CO)_7(PMe_3)_2$: decay to the baseline over a period of about 1.6 s, second-order rate behavior, and much more rapid, pseudo-first-order decay in the presence of CO. In the presence of $HSnBu_3$ (6.9×10^{-4} to 2.8×10^{-2} M), under Ar, the absorbance decays in several milliseconds to a level about half the original value, following first-order behavior, as illustrated in Figure 4. (It should be noted that the kinetics data were all obtained from solutions subjected to only one flash, because a significant fraction of the starting material is converted to product in a single flash.) Figure 5 shows a graph of the observed

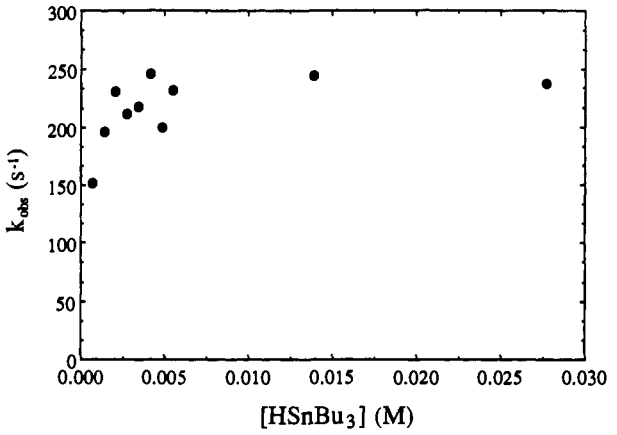

Figure 5. Variation in the pseudo-first-order rate constant, k_{obs}, for decays of absorption due to $Mn_2(CO)_7(PMe_3)_2$* as a function of $[HSnBu_3]$.

first-order rate constant for the transient decay as a function of $[HSnBu_3]$. The dependence is substantially nonlinear; there appears to be a saturation effect at a $HSnBu_3$ concentration of about 5×10^{-3} M.

The intermediate formed in the initial reaction of $Mn_2(CO)_7(PMe_3)_2$ with $HSnBu_3$ disappears over a period of approximately 2 s, following a first-order rate law. The derived rate constant of 1.6 (±0.3) s^{-1}, based on 11 determinations at varying concentrations of $HSnBu_3$, is independent of $[HSnBu_3]$.

$Mn_2(CO)_8[P(n\text{-}Bu)_3]_2$. The transient behavior of $Mn_2(CO)_8[P(n\text{-}Bu)_3]_2$ following flash photolysis was monitored at 540 nm. In the absence of $HSnBu_3$, under Ar, the transient absorption exhibits a small absorbance change over a period of milliseconds and then the expected slower decay ascribed to reaction of the CO-loss product $Mn_2(CO)_7[P(n\text{-}Bu)_3]_2$ with CO. The origin of the faster transient behavior is not clear; it may be due to some intramolecualr rearrangement of the phosphine ligands following CO loss. In the presence of $HSnBu_3$, under Ar, the transient decays over a period of several milliseconds to a small residual absorbance. Figure 6 shows a transient decay, the pseudo-first-order fit to the data, and the dependence of the pseudo-first-order rate constant on $[HSnBu_3]$. As with $Mn_2(CO)_7(PMe_3)_2$, the dependence on $[HSnBu_3]$ is decidedly nonlinear, and appears to saturate at a $HSnBu_3$ concentration around 0.03 M.

The product of the initial decay process is presumed to be the oxidative addition product $(CO)_4[P(n\text{-}Bu)_3]Mn\text{-}Mn(CO)_3[P(n\text{-}Bu)_3](H)(SnBu_3)$. It does not have a large absorbance at 540 nm. Nevertheless, the small absorbance that does remain can be observed to decay in less than 1 s, obeying a first-order rate law. The process at work here is reductive elimination of $HMn(CO)_4P(n\text{-}Bu)_3$, which leads also to a second product, $HMn(CO)_3[P(n\text{-}Bu)_3](SnBu_3)_2$, and smaller amounts of $Bu_3SnMn(CO)_4[P(n\text{-}Bu)_3]$, as determined from the continuous photolysis studies.[1] The rate constant for the slower process is estimated to be 5 (±1) s^{-1}.

Decay of the absorbance at 830 nm, assigned to the $Mn(CO)_4P(n\text{-}Bu)_3$· radical, was examined in the absence of $HSnBu_3$ and in the presence of 5.8×10^{-3} M $HSnBu_3$. In both cases the absorbances disappear via a second-order process. No change in the rate of decay of the absorbance was noted in the presence of $HSnBu_3$, in agreement with the conclusion from the continuous photolysis studies that the reaction of the dinuclear manganese compounds with $HSnBu_3$ occurs predominantly via oxidative addition to the CO-loss product.

$Mn_2(CO)_8[P(i\text{-}Bu)_3]_2$. The transient absorbance following flash photolysis of $Mn_2(CO)_8[P(i\text{-}Bu)_3]_2$ was observed at 560 nm. Under Ar in the absence of $HSnBu_3$ there is a rapid, small change in absorbance similar to that observed with $Mn_2(CO)_7[P(n\text{-}Bu)_3]_2$, followed by a slow decay over nearly 10 s, due to recombination with CO. In the presence of $HSnBu_3$ at concentrations ranging from 4×10^{-3} to 4×10^{-2} M, the absorbance decays to the baseline following a pseudo-first-order rate law, as illustrated in Figure 7a. In this case, a second, longer lived intermediate is not seen. Figure 7b also shows the dependence of the pseudo-first-order rate constant on $[HSnBu_3]$. From this linear dependence, a bimolecular rate constant of 1.7×10^4 M^{-1} s^{-1} is obtained.

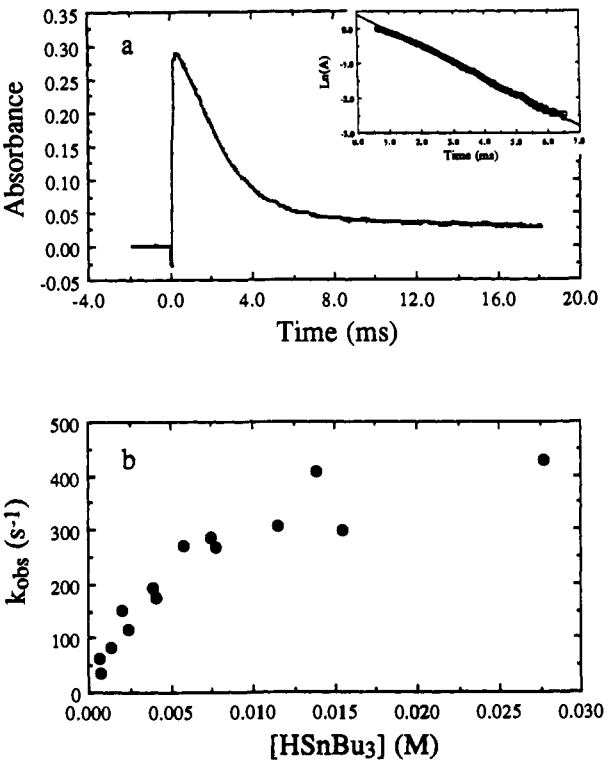

Figure 6. (a) Decay of the absorption at 540 nm following flash photolysis of a hexane solution under Ar, containing 1×10^{-4} M $Mn_2(CO)_8[P(n\text{-}Bu_3]_2$ and 1.3×10^{-2} M $HSnBu_3$. The inset shows the fit to a first-order decay, yielding k_{obs}. (b) Variation in k_{obs} for $Mn_2(CO)_7[P(n\text{-}Bu)_3]_2$* decay as a function of $[HSnBu_3]$.

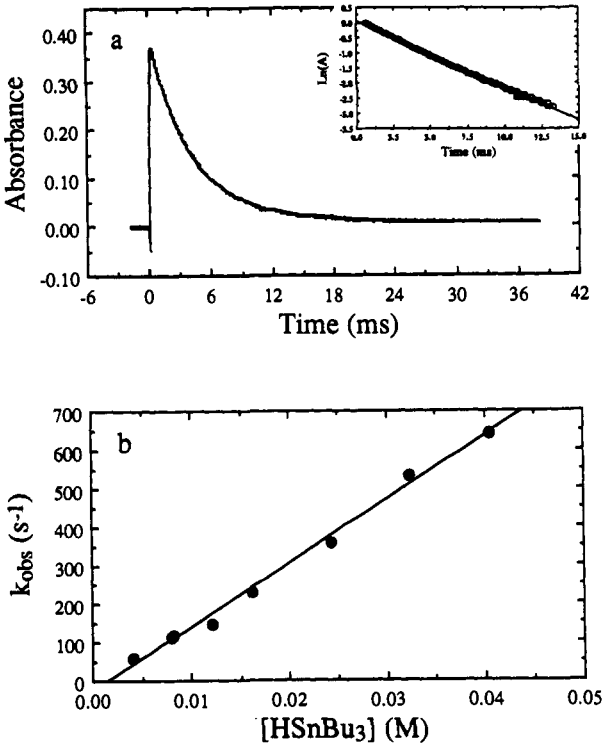

Figure 7. (a) Decay of the transient absorbance at 560 nm following flash photolysis of a hexane solution under Ar containing 1.0×10^{-4} M $Mn_2(CO)_8[P(i\text{-}Bu)_3]_2$ and 1.6×10^{-2} M $HSnBu_3$. The inset shows the fit to a first-order rate law. (b) Variation of k_{obs} for $Mn_2(CO)_7[P(i\text{-}Bu)_3]_2$ as a function of $[HSnBu_3]$.

The absorbance at 840 nm due to the $Mn(CO)_4P(i\text{-}Bu)_3$• radical was also observed, in both the presence and absence of $HSnBu_3$. The decays obey second-order kinetics and are unaffected by the presence of the hydride.

$Mn_2(CO)_8[P(i\text{-}Pr)_3]_2$ and $Mn_2(CO)_8[P(C_6H_{11})_3]_2$. The decay of the transient absorbance following flash photolysis of $Mn_2(CO)_8[P(i\text{-}Pr)_3]_2$ was monitored at 550 nm. The behavior of this system was entirely analogous to $Mn_2(CO)_8[P(i\text{-}Bu)_3]_2$, except that there was no evidence of the small, rapid change in transient absorbance in the absence of $HSnBu_3$. From the dependence of the pseudo-first-order rate constants on $[HSnBu_3]$, a value for the bimolecular rate constant of 1.05 (±0.04) × 10^2 M^{-1} s^{-1} was obtained. The transient at 780 nm due to the radical showed no effects from the presence of $HSnBu_3$.

The behavior of $Mn_2(CO)_8[P(C_6H_{11})_3]_2$ was entirely analogous to $Mn_2(CO)_8[P(i\text{-}Pr)_3]_2$. A bimolecular rate constant of 69 (±6) M^{-1} s^{-1} was obtained for the decay process.

$Mn_2(CO)_8[P(O\text{-}i\text{-}Pr)_3]_2$. When $Mn_2(CO)_8[P(O\text{-}i\text{-}Pr)_3]_2$ is flash photolyzed under 1 atm of Ar in hexane, a transient absorbance at 510 nm is observed. It decays slowly to the baseline in the manner expected for a CO-loss product. In contrast to the systems described thus far, when $HSnBu_3$ is present, the absorbance at 510 nm *increases* over a few milliseconds following the flash. At 580 nm a slight decrease in absorbance is observed in the same time interval. The product of the oxidative addition evidently has a rather similar absorbance spectrum to the CO-loss product. It was therefore difficult to obtain reliable kinetics results for the oxidative addition step. Assuming that the process is bimolecular, the bimolecular rate constant for reaction with $HSnBu_3$ is 1 × 10^4 M^{-1} s^{-1}.

The decay of the absorbance due to the oxidative addition product occurs over a period of about 6 s, and obeys a first-order rate law. The rate constant is independent of $[HSnBu_3]$; the average rate constant was determined to be 5.1 (±0.2) × 10^{-1} s^{-1}. The transient behavior of the absorbance at 780 nm due to the $Mn(CO)_4P(O\text{-}i\text{-}Pr)_3$• radical is unaffected by the presence of $HSnBu_3$.

B. Reactions of $Mn_2(CO)_{10}$ with $HSiEt_3$, $HSi(C_6H_5)_3$, and C–H Donors. When hexane solutions of $Mn_2(CO)_{10}$ containing $HSiEt_3$ (4×10^{-4} to 6×10^{-2} M) under Ar are flashed, the decay of the absorbance at 520 nm behaves as shown in Figure 8a. The absorbance remaining after 20 ms decays over a much longer period of time, as shown in Figure 8b. The behavior of the system is thus ostensibly very similar to the reaction with $HSnBu_3$. In both cases the transients disappear via a first-order rate law, although the slow process was not followed for sufficient time to test other forms of rate law. The pseudo-first-order rate constant of about 3×10^2 s^{-1} for the faster process did not vary significantly for $HSiEt_3$ concentrations in the range 3.8×10^{-2} to 6.3×10^{-2} M.

We interpret the initial change in absorbance as formation of the addition product $(CO)_5Mn\text{–}Mn(CO)_4(H\text{–}SiEt_3)$. Because this product is comparatively long-lived, it was possible to obtain an FTIR spectrum. The spectrum obtained following 10 s of irradiation with a 100-W tungsten lamp shows a single prominent absorption assigned to $HMn(CO)_5$, and others assigned to the oxidative addition product $(CO)_5Mn\text{–}Mn(CO)_4(H\text{–}SiEt_3)$. Over time these bands decrease in intensity, with comcommitant increases in the bands assigned to $Mn_2(CO)_{10}$. Changes in the absorbances due to $HMn(CO)_5$ are difficult to detect because of overlaps with bands due to $Mn_2(CO)_{10}$, but it can be said that most of the loss in $(CO)_5Mn\text{–}Mn(CO)_4(H\text{–}SiEt_3)$ appears as an increase in $Mn_2(CO)_{10}$.

The major difference between the $HSiEt_3$ and $HSnBu_3$ reactions thus lies in the products of the slower elimination step. Whereas with $HSnBu_3$ reductive elimination proceeds to form predominantly $HMn(CO)_5$ and either $HMn(CO)_4(SnBu_3)_2$ or $Bu_3SnMn(CO)_5$, $(CO)_5Mn\text{–}Mn(CO)_4(H\text{–}SiEt_3)$ yields mainly $HSiEt_3$; that is, the reaction simply reverses. A further illustration of the distinction between the two systems is that after eight flashes of the $HSiEt_3$-containing solutions, only a small amount of $HMn(CO)_5$ has formed, with corresponding slight decreases in absorbances due to $Mn_2(CO)_{10}$. By contrast, in solutions containing $HSnBu_3$, about 20% of the $Mn_2(CO)_{10}$ has converted to products after only one flash. Thus, elimination of $HSiEt_3$ competes strongly with reductive elimination of $HMn(CO)_5$, largely as a result of the larger bond energy for the H–Si bond, about 90 kcal mol^{-1},[21] as compared with H–Sn, 74 kcal mol^{-1}.[22]

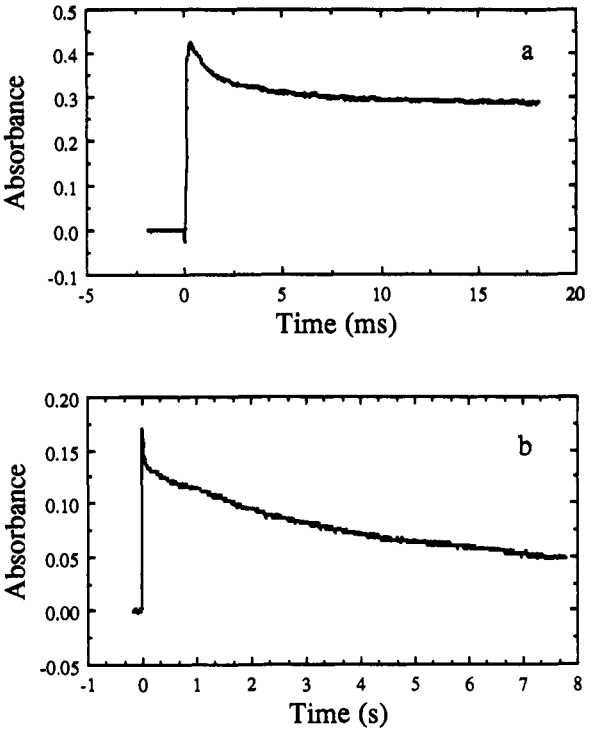

Figure 8. Absorbance at 520 nm following flash photolysis of hexane solutions under Ar containing 1.0×10^{-4} M $Mn_2(CO)_{10}$ and 5.0×10^{-2} M $HSiEt_3$: (a) millisecond time regime; (b) longer term decay.

It was noted in the preceding paper in this issue dealing with continuous photolysis that $Mn_2(CO)_{10}$ does not appear to undergo reaction with putatively strong H atom donors such as fluorene, triphenylmethane or triphenylsilane.[1] We found that the presence of any one of these compounds had no significant effect on the transient absorptions due to either $Mn_2(CO)_9$ or $Mn(CO)_5$. It is significant that all three of these compounds possess bond dissociation energies lower than that for $HSiEt_3$ (80, 81, and 86 kcal mol^{-1}, respectively, for fluorene,[23] triphenylmethane,[23] and triphenylsilane[24]). The failure to undergo oxidative addition must be ascribed to a steric impediment to attaining an appropriate transition-state geometry.

Discussion

The reactions of the CO-loss products $Mn_2(CO)_7L_2$ (L = CO, PMe_3, $P(n\text{-}Bu)_3$, $P(i\text{-}Bu)_3$, $P(i\text{-}Pr)_3$, $P(C_6H_{11})_3$, or $P(O\text{-}i\text{-}Pr)_3$) with $HSnBu_3$ can be thought of in a somewhat oversimplified way as an A → B → C type process, with the A → B step corresponding to oxidative addition of $HSnBu_3$

$$Mn_2(CO)_7L_2 + HSnBu_3 \rightarrow (CO)_4LMn\text{–}Mn(CO)_3L(H)(SnBu_3) \quad (2)$$

and the B → C step corresponding to reductive elimination

$$(CO)_4LMn\text{–}Mn(CO)_3L(H)(SnBu_3) \rightarrow HMn(CO)_4L + Bu_3SnMn(CO)_3L \quad (3)$$

The relative rates of oxidative addition and reductive elimination

(21) Kanaubus-Kaminski, J. M.; Hawari, J.; Griller, D. *J. Am. Chem. Soc.* **1987**, *109*, 5267.
(22) Jackson, R. A. *J. Organomet. Chem.* **1979**, *166*, 17.
(23) Bordwell, F. G.; Cheng, J.-P.; Harrelson, J. A., Jr. *J. Am. Chem. Soc.* **1988**, *110*, 1229.
(24) Dies, A. R.; Diogo, H. P.; Griller, D.; Minas da Piedade, M. E.; Martinho Simoes, G. A. In *Bonding Energetics in Organometallic Compounds*; Marks, T. J., Ed.; ACS Symposium Series 428; American Chemical Society: Washington, DC, 1990.

determine the character of the transient behavior. In one limiting case, corresponding to ligands of small steric requirement, $k_{ox}[HSnBu_3] \gg k_{red}$. In the other, corresponding to bulky ligands, the converse inequality applies. In the latter situation, no significant accumulation of the oxidative addition product is observed, and the rate of the final product formation is limited by the rate of oxidative addition of $HSnBu_3$ to $Mn_2(CO)_7L_2$.

The changeover from $k_{ox}[HSnBu_3] \gg k_{red}$ to $k_{ox}[HSnBu_3] \ll k_{red}$ occurs in part because the oxidative addition step is slower as the crowding around the coordinatively unsaturated metal center increases, and in part because increased ligand size (and probably also increased electron donation to the metal center) cause a more rapid reductive elimination to form $HMn(CO)_4L$ and the other observed products. Although several details must be added to the model for the reaction system to fully account for all our observations (vide infra), the important fundamental observation remains: *The lifetimes of the intermediates formed upon photochemical reaction of $HSnBu_3$ with $Mn_2(CO)_8L_2$ vary over a wide range, being long-lived for small ligands L, and increasingly short as ligand steric requirement and electron donor strength increase.* This observation, which does not emerge from the continuous photolysis results, has important implications for the potential for reaction of the intermediates with any substrates such as olefins or organic carbonyl compounds that might be present in the solution.

Mechanistic Analysis. A mechanistic scheme for the reactions under consideration here must take account of known or reasonably inferred properties of the metal carbonyl compounds: (1) The site of CO loss in the dinuclear species could, upon thermal equilibration, be occupied by a solvent molecule, by analogy with the mononuclear carbonyl systems such as $Cr(CO)_5$. (2) In noncoordinating solvents such as hexane, the coordinated solvent is displaced in favor of formation of the semibridging structure I. Although there is no direct evidence for the semibridging form in $Mn_2(CO)_7L_2$ where L is other than CO, the consistent behavior of the systems with respect to reaction with CO,[17a] and the observation that the one stable, isolated semibridging molecule has phosphines bound to the metal,[16] suggest that in noncoordinating solvents the semibridging form is general for $Mn_2(CO)_7L_2$. (3) Oxidative addition of $HSnBu_3$ to the Mn center may occur in a separate, slower step, following addition of $HSnBu_3$ to the site.

A detailed mechanistic scheme must account for the products of the reactions and variations in observed rates with changes in L. It must also account for the dependence of observed rate constants on concentrations, in particular the nonlinear variation in the observed rate constant for oxidative addition with $HSnBu_3$ concentration in the PMe_3 and $P(n\text{-}Bu)_3$ cases.

Scheme I shows a comprehensive reaction scheme that embodies the properties alluded to above.

Scheme I

$$Mn_2(CO)_7L_2 + S\ (=\text{solvent}) \underset{k_2}{\overset{k_1}{\rightleftharpoons}} Mn_2(CO)_7L_2(S) \quad (4)$$

$$Mn_2(CO)_7L_2 \underset{k_4}{\overset{k_3}{\rightleftharpoons}} Mn_2(CO)_7L_2^*\ (^* \text{ denotes semibridging form}) \quad (5)$$

$$Mn_2(CO)_7L_2 + HSnBu_3 \underset{k_6}{\overset{k_5}{\rightleftharpoons}} Mn_2(CO)_7L_2(HSnBu_3) \quad (6)$$

$$Mn_2(CO)_7L_2(HSnBu_3) \underset{k_8}{\overset{k_7}{\rightleftharpoons}} Mn_2(CO)_7L_2(H)(SnBu_3) \quad (7)$$

$$Mn_2(CO)_7L_2(H)(SnBu_3) \xrightarrow{k_9} HMn(CO)_5 + Bu_3SnMn(CO)_4 \quad (8)$$

$$Bu_3SnMn(CO)_4 + CO \xrightarrow{k_{10}} Bu_3SnMn(CO)_5 \quad (9)$$

$$Bu_3SnMn(CO)_4 + HSnBu_3 \xrightarrow{k_{11}} HMn(CO)_4(SnBu_3)_2 \quad (10)$$

In terms of kinetics analysis, the reaction scheme can be simplified by several considerations. Because our concern is only with the comparatively rapid early steps of the reaction, we can ignore steps 8–10. Further, the oxidative addition of $HSnBu_3$ to Mn should be strongly exergonic, given that the Sn–H bond energy is 74 kcal mol^{-1}, and that the Mn–H and Mn–Sn bond energies are likely to lie in the ranges of 65 kcal mol^{-1} [25] and 47 kcal mol^{-1},[26] respectively. We further expect that dissociation of $HSnBu_3$ from the metal center, the reverse reaction in eq 6, would be perhaps 10 kcal mol^{-1} or more endergonic, by analogy with the enthalpies of dissociation of alkanes[27] and silanes[28] from $Cr(CO)_5$. There is no reason to anticipate a significant barrier to the oxidative addition process. Thus, k_7 should be much larger than k_6, and we can ignore the $HSnBu_3$ dissociation process, as well as the reverse reaction in eq 7. This is equivalent to assuming that oxidative addition of $HSnBu_3$ occurs in a single, concerted step.

In the flash photolysis experiment in hydrocarbon solvent, we observe the disappearance of $Mn_2(CO)_7L_2^*$:

$$-d[Mn_2(CO)_7L_2^*]/dt = -k_4[Mn_2(CO)_7L_2^*] + k_3[Mn_2(CO)_7L_2] \quad (11)$$

Assuming that the steady-state assumption can be applied to the intermediates $Mn_2(CO)_7L_2$, $Mn_2(CO)_7L_2(S)$, and $Mn_2(CO)_7L_2(HSnBu_3)$, we obtain

$$\frac{-d[Mn_2(CO)_7L_2^*]}{dt} = \frac{k_4k_5k_7[HSnBu_3][Mn_2(CO)_7L_2^*]}{\{k_3(k_6 + k_7) + k_5k_7[HSnBu_3]\}} \quad (12)$$

In the presence of excess $HSnBu_3$, the oxidative addition process is observed to be pseudo-first-order. Therefore

$$-d[Mn_2(CO)_7L_2^*]/dt = k_{obs}[Mn_2(CO)_7L_2^*] \quad (13)$$

$$k_{obs} = \frac{k_4k_5k_7[HSnBu_3]}{\{k_3(k_6 + k_7) + k_5k_7[HSnBu_3]\}} \quad (14)$$

For $k_7 \gg k_6$

$$k_{obs} = \frac{k_4k_5[HSnBu_3]}{k_3 + k_5[HSnBu_3]} \quad (15)$$

In the mechanistic scheme adopted, it is assumed that only the open, or naked Mn center can react with either solvent, a CO group on the adjacent Mn, or $HSnBu_3$. This model is consistent with much recent work on displacement of loosely bound, or "token", ligands from Cr in $Cr(CO)_5$.[15]

The solvent interaction with $Mn_2(CO)_7L_2$ does not appear in the steady-state approximation expression for k_{obs}. This is a consequence of the fact that the semibridging form is more stable than the solvated form. Most importantly, it should be noted that if $k_3 \gg k_5[HSnBu_3]$, k_{obs} increases linearly with $[HSnBu_3]$, in contrast to the experimental results for $Mn_2(CO)_8(PMe_3)_2$ and $Mn_2(CO)_8[P(n\text{-}Bu)_3]_2$, in which k_{obs} approaches a limiting value. In terms of this model, therefore, the kinetics results suggest that formation of the semibridging form is an activated process. This activation does not consist in the activation enthalpy for solvent dissociation; that has already been accounted for in the model. Rather, it is an activation energy required to form the semibridged form from the open form of $Mn_2(CO)_7L_2$. A simple way of viewing the point is this: Assuming that $HSnBu_3$ reacts only at the open site, it competes for this site with solvent and the CO group that forms the semibridge. The competition with solvent drops out, because the semibridging form is the more stable, predominant species in solution. If the bridge on–off equilibrium were very fast ($k_3 \gg k_5[HSnBu_3]$), k_{obs} would simply vary linearly with $[HSnBu_3]$. For there to be a real kinetic competition, k_3 and $k_5[HSnBu_3]$ must be of comparable magnitudes.

(25) (a) Tilset, M.; Parker, V. D. *J. Am. Chem. Soc.* **1989**, *111*, 6711. (b) Eisenberg, D. C.; Norton, J. R. *Isr. J. Chem.*, in press. (c) Brown, T. L. In *Organometallic Radical Processes*; Trogler, W., Ed.; Elsevier Press: Amsterdam, 1990; p 100.

(26) Harris, D. H.; Spalding, T. R. *Inorg. Chim. Acta* **1980**, *39*, 187.

(27) (a) Morse, J., Jr.; Parker, G.; Burkey, T. J. *Organometallics* **1989**, *8*, 2471. (b) Yang, G. K.; Vaida, V.; Peters, K. S. *Polyhedron* **1988**, *7*, 1619.

(28) Burkey, T. J. *J. Am. Chem. Soc.* **1990**, *112*, 8329.

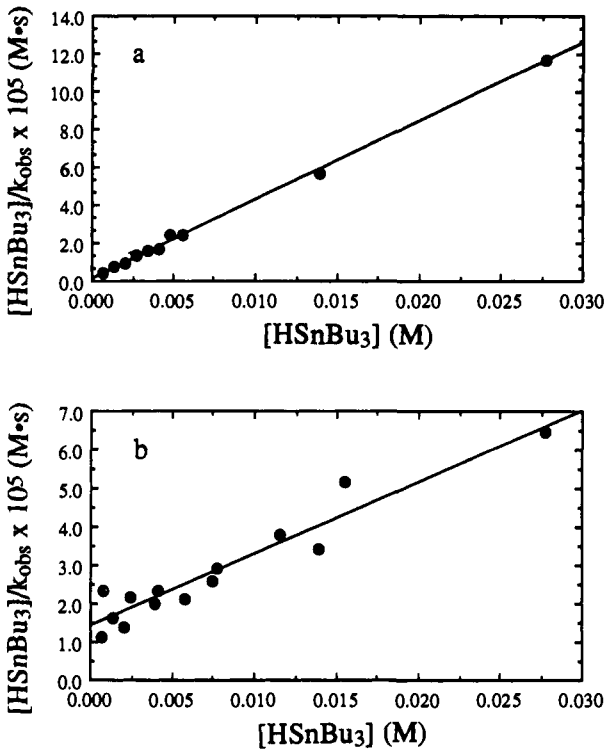

Figure 9. $[HSnBu_3]/k_{obs}$ vs $[HSnBu_3]$ for (a) $Mn_2(CO)_8(PMe_3)_2$ and (b) $Mn_2(CO)_8[P(n\text{-}Bu)_3]_2$.

Table I. Values for Rate Constants Assumed in Numerical Modeling

rate constant	$Mn_2(CO)_8(PMe_3)_2$ reaction	$Mn_2(CO)_8[P(n\text{-}Bu)_3]_2$ reaction
k_1 (M^{-1} s^{-1})	1×10^9	1×10^8
k_2 (s^{-1})	1×10^8	1×10^7
k_3 (s^{-1})	1.6×10^5	7.0×10^5
k_4 (s^{-1})	2.5×10^2	5.5×10^2
k_5 (M^{-1} s^{-1})	3×10^8	1×10^8

Rearrangement of eq 15 lead to eq 16. Figure 9 shows plots of $[HSnBu_3]/k_{obs}$ vs $[HSnBu_3]$ for $Mn_2(CO)_8(PMe_3)_2$ and $Mn_2(CO)_8[P(n\text{-}Bu)_3]_2$. In both cases the data fit the expected

$$[HSnBu_3]/k_{obs} = k_4^{-1}[HSnBu_3] + k_3/k_4k_5 \qquad (16)$$

linear relationship reasonably well. From the slopes we obtain values for k_4 of 2.42 (±0.07) $\times 10^2$ s^{-1} for $Mn_2(CO)_8(PMe_3)_2$ and 5.3 (±0.8) $\times 10^2$ s^{-1} for $Mn_2(CO)_8[P(n\text{-}Bu)_3]_2$. It is encouraging that these two values are not much different from one another, in spite of the substantially different appearances of the data as shown in Figures 5 and 6. Since we do not know the value of k_5, we cannot obtain a value of k_3 from the intercept. However, it is possible to estimate this value by numerical modeling of the reaction system.

Numerical Modeling. We have employed numerical integration of the rate equations, using the HAVCHM program,[29] to model the kinetics behavior of the $Mn_2(CO)_8(PMe_3)_2$ and $Mn_2(CO)_8[P(n\text{-}Bu)_3]_2$ reactions. Values were assumed for k_1 and k_5. For each set of assumed rate constants, the computed rate of disappearance of $Mn_2(CO)_7L_2$* followed a pseudo-first-order rate law. The value of this computed k_{obs} was then calculated as a function of $[HSnBu_3]$ and compared with experimental data.

The values selected for k_1 and k_2 were constrained so that $k_1/k_2 \ll k_3/k_4$, in keeping with the assumption that the semibridging form is the predominant form in solution. In analogy with the work done on $Cr(CO)_5$, one would expect k_1 to be quite large. Table I lists the values for the rate constants that led to good numerical agreement with the experimental observations. Figure 10 shows the calculation variations in k_{obs} vs $[HSnBu_3]$ based on

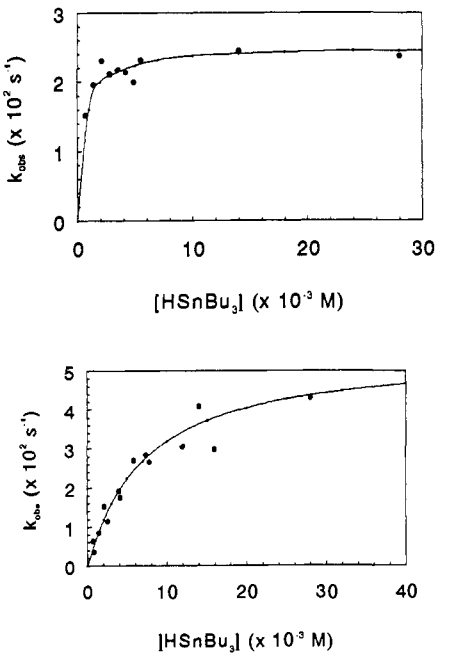

Figure 10. Comparison of k_{obs} vs $[HSnBu_3]$ from numerical simulation (lines) with experimental data (circles): (a) $Mn_2(CO)_8(PMe_3)_2$; (b) $Mn_2(CO)_8[P(n\text{-}Bu)_3]_2$.

those rate constants. The intent of the simulation is to show that, without resort to the steady-state approximation, a reasonable fit to the kinetics observations is achieved for values of k_3 that imply a significant free energy barrier for formation of the semibridged intermediate.

While the precision of the estimated rate constants is not high, the most critical quantities k_3, k_4, and k_5 are constrained to rather narrow limits by the fits to experiment. The value for k_4 in the simulation determines in large measure the limiting value attained by k_{obs}. The fit to this parameter in the simulations is thus quite sensitive, and not especially influenced by variations in the values chosen for other rate constants.

The values assumed for the ratio k_5/k_3 in the simulations affect the curvature in the plots of k_{obs} vs $[HSnBu_3]$, and the range of $[HSnBu_3]$ in which the limiting value is obtained. We chose values for k_5 of 3×10^8 and 1×10^8 M^{-1} s^{-1} for $Mn_2(CO)_8(PMe_3)_2$ and $Mn_2(CO)_8[P(n\text{-}Bu)_3]_2$, respectively. These are conservative choices, in the sense that they are as large as seem reasonable, thus leading to the largest reasonable estimates for k_3. The value of k_3 that leads to best agreement with the observations is 1.6×10^5 s^{-1} for $Mn_2(CO)_8(PMe_3)_2$ and 7.0×10^5 for $Mn_2(CO)_8[P(n\text{-}Bu)_3]_2$. The former value is in good agreement with the value of 2.4×10^5 M^{-1} s^{-1} estimated for $Mn_2(CO)_8(PMe_3)_2$ from continuous photolysis results.[1]

If there were no free energy barrier to formation of the semibridged form from the open form, the value for k_3 should be on the order of magnitude of a bending frequency, 10^{13} s^{-1}. The estimates for k_3 from the simulations and steady-state treatments are several orders of magnitude smaller than this, suggesting a significant barrier to formation of the semibridge. The factor of about 10^6–10^7 in rate constant represents a free energy barrier in the range of 8–10 kcal mol^{-1}. It is not surprising that there should be a barrier, since there must be some distortion away from an equilibrium geometry about the 18-electron Mn center before the CO group can approach the open metal center for bonding to take effect. In $Mn_2(CO)_{10}$ the angle between trans-equatorial CO groups is about 170°.[30] A substantially smaller angle must obtain in the semibridging form. In $Mn_2(CO)_5(dppm)_2$, the C_{br}–Mn–C angle with the trans CO group is only 132°.[16]

If formation of the semibridging form from the open form is indeed activated, the question arises as to how rapidly the semi-

(29) (a) Stabler, R. N.; Chesick, J. P. *Int. J. Chem. Kinet.* **1978**, *10*, 461. (b) Chesick, J. P. *J. Chem. Educ.* **1988**, *65*, 599.

(30) Dahl, L. F.; Rundle, R. E. *Acta Crystallogr.* **1963**, *16*, 419.

Table II. Apparent Rate Constants, k_{add}, for Oxidative Addition of $HSnBu_3$ to $Mn_2(CO)_7L_2$

ligand	k_{add} (M^{-1} s^{-1})	cone angle[31] (deg)
CO	2.5×10^6	95
PMe_3	3×10^5	118
$P(n\text{-}Bu)_3$	8×10^5	132
$P(i\text{-}Bu)_3$	1.7×10^4	143
$P(i\text{-}Pr)_3$	1.0×10^2	160
$P(C_6H_{11})_3$	69	170
$P(O\text{-}i\text{-}Pr)_3$[a]	1×10^4	130

[a] Because the form of the rate law was not confirmed, this estimate could be in error.

bridging species forms following the primary CO-loss photoprocess. In this circumstance, the $Mn_2(CO)_9$ initially formed is likely to possess considerable excess energy. Over a period of tens of picoseconds it cools through energy-transferring collisions with solvent molecules. At some stage during the cooling process the molecule will possess sufficient excess energy to facilitate the unimolecular process leading to formation of the semibridge, followed by trapping in this form as the molecule cools further. On the other hand, if the molecule passes through this regime of excess energy without formation of the semibridge, the vacancy at the metal center is most likely to be captured initially by solvent. Formation of the semibridged form from the solvated form might then be expected to require on the order of microseconds.

We have no knowledge of the kinetics of formation of the semibridged form following the flash. In the hopes that there might be significant differences in the UV–visible spectra of $Mn_2(CO)_7L_2(S)$ and $Mn_2(CO)_7L_2$*, we have searched for variations in the transient spectra observed following laser flash photolysis of $Mn_2(CO)_{10}$ in hexane under Ar, using a N_2 laser with a 10–20-ns pulse width. We have not been able to reliably identify such changes.[31] We also studied $Mn_2(CO)_8(PMe_3)_2$, in which changes in the transient spectra in the time domain in question have been reported.[32] However, it was not possible to associate the transient behavior unambiguously with formation of the semibridging form. The most reasonable hypothesis at present seems to be that the semibridged species is formed to a large extent in the short time interval following the flash. However, our kinetics analysis and conclusions do not require this assumption.

(31) In their study of the gas-phase photodissociation pathways for $Mn_2(CO)_{10}$, Weitz et al. observe a transient IR absorption at 1745 cm^{-1} which they ascribe to semibridging $Mn_2(CO)_9$.[17b] The absorption is present within several microseconds.

(32) Yasufuku, K.; Hiraga, N.; Ichimara, K.; Kobayashi, T. *Coord. Chem. Rev.* **1990**, *97*, 167.

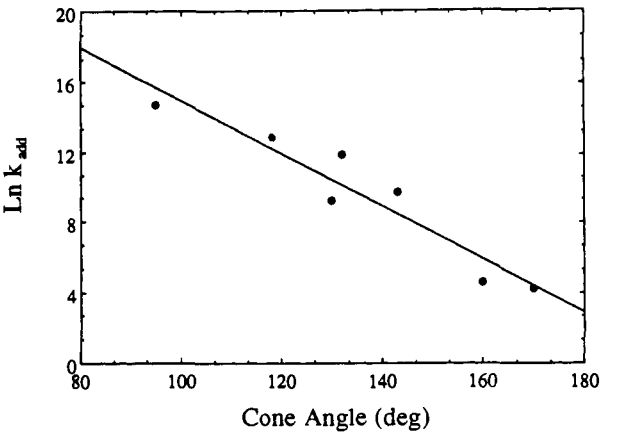

Figure 11. ln k_{add} vs cone angle ($k_{add} = k_4k_5/k_3$).

Ligand Effects. It is evident that ligand size materially affects the rate at which $HSnBu_3$ adds to $Mn_2(CO)_7L_2$. For ligands larger than $P(n\text{-}Bu)_3$, k_{obs} varies linearly with $[HSnBu_3]$. From eq 15, a linear relationship should obtain when $k_3 \gg k_5[HSnBu_3]$. Under these conditions, the slope of the plot of k_{obs} vs $[HSnBu_3]$ corresponds to $k_{add} = k_4k_5/k_3$. This quantity grows smaller as the steric requirement of the ligand increases.

The value for k_{add} can be estimated for $Mn_2(CO)_{10}$ from the continuous photolysis studies as 2.5×10^6 M^{-1} s^{-1}.[1] For $Mn_2(CO)_8(PMe_3)_2$ and $Mn_2(CO)_8[P(n\text{-}Bu)_3]_2$, which exhibit nonlinear plots of $k_{obs}[HSnBu_3]$, k_{add} can be calculated from the values listed in Table I. The value obtained in this manner for $Mn_2(CO)_8(PMe_3)_2$, 4.7×10^5 M^{-1} s^{-1}, is larger than the value of 1.9×10^5 M^{-1} s^{-1} estimated from the continous photolysis work.[1] Neither value is very precisely determined; we adopt an average of the two values, 3×10^5 M^{-1} s^{-1}. The values of k_{add} for the remaining ligands are as indicated previously; all are listed in Table II. Figure 11 shows a graph of ln k_{add} vs the cone angle of the ligand L.[33] A reasonably good linear relationship ($R = 0.91$) is found. Not surprisingly, the conclusion from this correlation is that the oxidative addition of $HSnBu_3$ to the coordinatively unsaturated site in $Mn_2(CO)_7L_2$ is increasingly impeded as L increases in size. At the same time, the rate of reductive elimination apparently increases in the order $CO < P(O\text{-}i\text{-}Pr)_3 < PMe_3 < P(n\text{-}Bu)_3 < (P(i\text{-}Bu)_3, P(i\text{-}Pr)_3, P(C_6H_{11})_3)$.

Acknowledgment. This research was supported by the National Science Foundation through research Grants CHE86-08839 and CHE89-12773.

(33) Tolman, C. A. *Chem. Rev.* **1977**, *77*, 313.